

AD-A047 400

NAVAL RESEARCH LAB WASHINGTON D C  
STEADY-ABLATION MODEL OF ACCELERATING LASER-TARGET SLABS.(U)  
SEP 77 F S FELBER

F/G 20/5

UNCLASSIFIED

NRL-MR-3569

SBIE-AD-E000 017

NL

AD  
A047400

END  
DATE  
FILMED

1 -78

DDC

AD A047400



AD-E000 017  
NRL Memorandum Report 3569

## Steady-Ablation Model of Accelerating Laser-Target Slabs

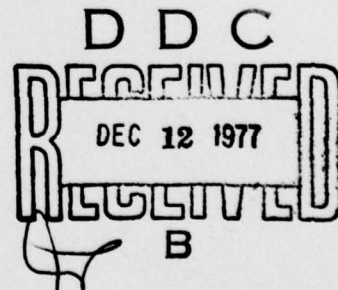
F. S. FELBER

*Laser Plasma Branch  
Plasma Physics Division*

September 1977



NAVAL RESEARCH LABORATORY  
Washington, D.C.



AD No. \_\_\_\_\_  
DDC FILE COPY

Approved for public release: distribution unlimited.

SECURITY CLASSIFICATION OF THIS PAGE (When Data Entered)

REPORT DOCUMENTATION PAGE		READ INSTRUCTIONS BEFORE COMPLETING FORM
1. REPORT NUMBER NRL Memorandum Report 3569	2. GOVT ACCESSION NO.	3. RECIPIENT'S CATALOG NUMBER
4. TITLE (and Subtitle) STEADY-ABLATION MODEL OF ACCELERATING LASER-TARGET SLABS	5. TYPE OF REPORT & PERIOD COVERED Interim report on a continuing NRL problem.	
7. AUTHOR(s) F.S. Felber	6. PERFORMING ORG. REPORT NUMBER	
9. PERFORMING ORGANIZATION NAME AND ADDRESS Naval Research Laboratory Washington, D.C. 20375	8. CONTRACT OR GRANT NUMBER(s)	
11. CONTROLLING OFFICE NAME AND ADDRESS Energy Research and Development Administration Washington, D.C. 20545	10. PROGRAM ELEMENT PROJECT, TASK AREA & WORK UNIT NUMBERS NRL Problem H02-29A	
14. MONITORING AGENCY NAME & ADDRESS (if different from Controlling Office) 12p.	12. REPORT DATE September 1977	
	13. NUMBER OF PAGES 13	
	15. SECURITY CLASS. (of this report) UNCLASSIFIED	
	15a. DECLASSIFICATION/DOWNGRADING SCHEDULE	
16. DISTRIBUTION STATEMENT (of this Report) Approved for public release; distribution unlimited. SBIE		
17. DISTRIBUTION STATEMENT (of the abstract entered in Block 20, if different from Report) AD-E0001017		
18. SUPPLEMENTARY NOTES *This work was supported by a National Research Council Resident Research Associateship at the Naval Research Laboratory.		
19. KEY WORDS (Continue on reverse side if necessary and identify by block number) Flat targets Ablation Laser-driven targets Steady-state ablation Laser-plasma interaction Transsonic flow Density profile modification Accelerating laser targets		
20. ABSTRACT (Continue on reverse side if necessary and identify by block number) A steady-state model of a plasma slab, accelerated by interaction with laser radiation, deter- mines temperature, velocity, and density profiles and boundaries consistent with laser intensity and wavelength, and slab mass and acceleration. Density profile modification is caused by laser pressure. Plasma flows subsonically into the critical surface, supersonically out.		

DD FORM 1 JAN 73 1473

EDITION OF 1 NOV 65 IS OBSOLETE  
S/N 0102-014-6601

SECURITY CLASSIFICATION OF THIS PAGE (When Data Entered)

251950

AB

SECURITY CLASSIFICATION OF THIS PAGE (When Data Entered)

SECRET

1. TITLE

2. AUTHOR

3. PERIODICITY

4. DATE

5. NUMBER

6. VOLUME

7. ISSUE

8. PAGE

9. TOTAL PAGES

10. ABSTRACT

11. SUMMARY

12. CONCLUSIONS

13. RECOMMENDATIONS

14. REFERENCES

15. NOTES

16. COMMENTS

17. INDEXING

18. KEYWORDS

19. SUBJECTS

20. DISTRIBUTION

21. AVAILABILITY

22. SECURITY

23. CLASSIFICATION

24. DECLASSIFICATION

25. OTHER



## STEADY-STATE MODEL OF A FLAT LASER-DRIVEN TARGET

In an earlier paper<sup>1</sup> exact transmission coefficients were calculated for intense light incident on a plasma slab in which ions were frozen. In this paper a steady-state model of a plasma slab, accelerated by its interaction with laser radiation, is treated by 1-D steady-flow hydrodynamic equations in an accelerated frame of reference. The cold unablated fluid, the ablation layer, both classical and flux-limited hot conduction regions, the critical surface, and the underdense blowoff are all considered. A global description determines the temperature, density, velocity, and boundaries as well. Approximate analytic solutions are given in each of the plasma regions.

The ablation layer, containing a steep density gradient separating cold dense fluid from hot low density plasma, moves at the front of the thermal wave and is accelerated by the rocket reaction to the ablation. Nevertheless J. Boris has demonstrated through time-dependent numerical simulations that the temperature profile at the ablation layer is steady in an accelerated reference frame, and has provided a simplified analytic model of the steady temperature profile at the ablation layer.<sup>2</sup>

The quasisteady-state model presented here accounts self consistently for the (slow) increase in acceleration of the slab owing to the diminishing mass of cold fluid being accelerated.

While a slab geometry reveals most of the important physics, and can be used to consider flat target experiments and instability at the ablation layer, the model readily transforms to a spherical geometry. Max et al.<sup>3</sup> have found analytic steady-state

Note: Manuscript submitted July 18, 1977.

White Section <input checked="" type="checkbox"/>	
Grey Section <input type="checkbox"/>	
<input type="checkbox"/>	
DISTRIBUTION/AVAILABILITY CODES	
Dist	and/or SPECIAL
A	

solutions for plasma flow in the hot conduction region of spherical laser targets, and Gitomer et al.<sup>4</sup> have treated spherical flow with an artificial mass source.

The model is formulated in terms of time-independent solutions of the continuity, momentum, and energy equations,

$$\begin{aligned} 0 &= \frac{\partial \rho}{\partial t} = - \frac{\partial}{\partial x} (\rho v) , \\ 0 &= \frac{\partial}{\partial t} (\rho v) = - \frac{\partial}{\partial x} (\rho v^2 + P) + \rho g - \left( \frac{I_a + 2I_r}{c} \right) \delta(x - x_c) , \\ 0 &= \frac{\partial \mathcal{E}}{\partial t} = - \frac{\partial}{\partial x} (Pv + \mathcal{E}v + q) + \rho g v + I_a \delta(x - x_c) . \end{aligned} \quad (1)$$

Here  $v$  is the velocity of a volume element of mass density  $\rho$ , temperature (in energy units)  $T$ , pressure  $P = \rho T/m_i$ , ion mass  $m_i$ , and local energy density  $\mathcal{E} = (3P + \rho v^2)/2$ ; absorbed (reflected) laser flux is  $I_a$  ( $I_r$ ).

The laser energy and momentum is regarded as deposited at the critical surface  $x = x_c$ . The momentum deposition term causes gradient steepening and density shelves at the critical surface that have been observed experimentally,<sup>5</sup> and calculated theoretically<sup>6</sup> by other means.

The effective gravity  $g$  must be included in the energy equation as the product of force density  $\rho g$  with velocity  $v$ . It cannot be omitted, as in Ref. 7.

The heat flux  $q$  at any point in the hot conduction region is considered to be the lesser in magnitude of the classical flux  $q_{\text{class}} = KT^{5/2}T'$  and limited flux  $q_{\text{lim}} = -\ell \rho (T/m_i)^{3/2} T'/|T'|$ . A prime denotes  $d/dx$ ,  $KT^{5/2}$  is conductivity, and the flux-limit parameter  $\ell$  lies in the author-dependent range<sup>3</sup>  $0.5 \leq \ell \leq 60$ . An upper bound,  $\ell \leq 3$ , for this model is derived below.

The continuity equation implies constant momentum density  $\rho v = \rho_0 v_0$ . Fluid quantities evaluated at the origin, chosen at the surface of

maximum density, are denoted by a subscript zero. Then the momentum and integrated energy equations in the overdense fluid simplify to two first order equations in  $\rho$  and  $T$

$$\begin{aligned} \rho' &= \rho(T' - m_i g) / [\Gamma m_i v_o^2 (\rho_o / \rho)^2 - T] , \\ q(T, T', \rho) &= - \frac{1}{2} (\rho_o v_o / m_i) [5(T - T_o) + m_i v_o^2 (\rho_o^2 / \rho^2 - 1) - 2m_i g x] \\ &\quad - K T_o^{5/2} m_i g , \end{aligned} \quad (2)$$

that can be solved by a Runge-Kutta code in classical-conduction and flux-limited regions. Solutions near the ablation layer are shown in Fig. 1.

The flux  $\sim T^{5/2} T'$  in the cold fluid rises monotonically towards the heat source, but the temperature gradient  $T'$ , while positive definite, is not necessarily monotonic. At maximum density,  $T' = m_i g$ ; conduction is enhanced by increased acceleration.

If the dimensionless gravity  $\Gamma \equiv (m_i^2 K T_o^{3/2} / \rho_o v_o) g$  and Mach number  $M \equiv (m_i v_o^2 / T)^{1/2}$  are both  $\ll 1$  in the cold fluid, then approximate analytic solutions of (2) are

$$\begin{aligned} T &\approx T_o (1 - 6\Gamma/25 + 2m_i g x / 5T_o) , \\ \rho &\approx \rho_o (1 + 3m_i g x / 5T_o) , \quad (-T_o / m_i g \leq x \leq 0) . \end{aligned} \quad (3)$$

Indeed the laminar ablation rate is generally much less than the local sound speed at the ablation layer in ablative implosions, though not in exploding-pusher targets.

A sonic point ( $M = 1$ ) can occur in the cold fluid at

$$x_s = \frac{T_o}{m_i g} \left[ \frac{5 + M_o^2}{2} + \Gamma \left( \frac{M_o \rho_o}{\rho(x_s)} \right)^5 - \Gamma - 3 \left( \frac{M_o \rho_o}{\rho(x_s)} \right)^2 \right] .$$

If  $M \ll 1$ , and  $\Gamma \ll 1$ , then an approximate analytic solution of (2) in the hot classically conducting region, valid for  $0 \leq x \leq T_0/m_1 g$  is

$$x(T) \approx \frac{4m_1 K T_0^{5/2}}{25 \rho_0 v_0} [\tau^{5/2} - 1] + \frac{5}{3} (\tau^{3/2} - 1) + 5 (\tau^{1/2} - 1), \quad (4)$$

in which  $\tau \equiv T/T_0$ . The analytic solutions (3) and (4) for cold and hot conduction regions are compared in Fig. 1 with the numerical solution of (2). At high temperatures (4) can be inverted

$$T \approx (25 \rho_0 v_0 / 4 m_1 K)^{2/5} x^{2/5} - 2T_0/3, \quad (T \gg T_0).$$

At sufficiently high temperature and low density, the heat flux may saturate in the overdense region. The solutions of (2) for both classical flux and saturated flux are matched where  $q_{\text{class}} = q_{\text{lim}}$ . In a saturated-flux region (2) implies<sup>3</sup>

$$(5 + M^2 - 2\ell/M)T = 2m_1 g x + (5 - 2\Gamma + M_0^2)T_0 \approx 2m_1 g x + 5T_0. \quad (5)$$

The gravity gives the Mach number a spatial dependence and boost; the flow is assisted, and onset of flux limiting delayed.

At the critical surface, conservation of mass requires  $\rho_+ v_+ = \rho_- v_-$ , so that the jumps in density and velocity are related by

$$v_+ \Delta \rho = - \rho_- \Delta v. \quad (6)$$

The notation concerning the jump in any variable  $u$  is defined by  $\Delta u \equiv u_+ - u_- \equiv u(x_c + 0) - u(x_c - 0)$ . All energy deposited at the critical surface is assumed to be conducted into the much more massive and colder overdense region, so that  $q = 0$  in the underdense region, and an adiabatic equation of state applies there. Then with  $\Delta T = 0$  and  $T(x_c) \equiv T_c$ ,  $\Delta q = -q(\rho_-, T_c) > 0$ . The jump conditions from (1) are



$$\Delta\rho = -m_i(I_a + 2I_r)/(T_c - m_i v_-^2 \varphi) c, \quad \Delta v = (\varphi - 1)v_-, \quad (7)$$

where  $\varphi \equiv [1 + 2(I_a - \Delta q)/\rho_- v_-^3]^{1/2}$ . The case is considered for which the heat conducted away from  $x_c$  does not exceed the laser energy deposited there, so that  $\varphi > 1$ . Together (6) and (7) imply

$$I_a + 2I_r = (\rho_- c/m_i)(T_c - m_i v_-^2 \varphi)(1 - 1/\varphi). \quad (8)$$

Since  $I_a + 2I_r > 0$  and  $\varphi > 1$ , then  $m_i v_-^2 < T_c$ . Thus steady flow into the critical surface is subsonic in the rest frame of the critical surface.<sup>9</sup> Then (5) implies the flux-limit parameter  $\lambda$  must be less than  $\beta$  for a flux-limited region to exist in steady state. This upper bound is comparable with recent experimental values and theoretical predictions.<sup>3,11</sup>

Mass, momentum and energy conservation across the critical surface insufficiently constrain the solution.<sup>6</sup> A reasonable added constraint derived in Ref. 6 for a related problem, and independent of ponderomotive force, is  $\rho_- = \rho_c [M_-^2 - \ln(M_-^2) - 1]/2(1 - M_-)^2$ . The density shelves and subsonic flow into the critical surface are features of other theoretical treatments<sup>6</sup> as well, and are seen here to be caused exclusively by laser momentum deposition.

Ordinarily a ponderomotive force term proportional to  $\rho d|E|^2/dx$  is appended to the momentum equation to model the effects of the electric field  $E$  in the underdense region, imposing spatially periodic fluctuations on density and velocity profiles. In this model the momentum equation is averaged over many wavelengths to iron out the effects of the ponderomotive force,  $\langle \rho d|E|^2/dx \rangle_x = 0$ , and leave only the gross profiles of the steady flow of an ideal, adiabatic gas in the underdense region.

The exact solutions of (1) for the underdense, adiabatic gas are

$$v^2 - 5(T_c/m_i)[1 - (v_+/v)^{2/3}] = v_+^2 + 2g(x - x_c) \quad (9)$$

$$\rho = \rho_+ v_+/v, \quad T = T_c (v_+/v)^{2/3}$$

On physical grounds  $T$  must decrease away from the heat source at  $x_c$ . Then (9) implies the flow out of the critical surface must be supersonic,  $m_i v_+^2 > 5T_c/3$ .

The gravity determines the boundaries self consistently. Let the total plasma mass per area,  $m$ , be specified. Since momentum density is uniform, during a time  $\delta t$ , a thin layer of mass  $\delta m = \rho_L v_L \delta t = \rho_- v_- \delta t$  is effectively transferred from the left boundary  $x_L$  to the right boundary  $x_R$  at higher velocity  $v_R$ . The change in momentum,  $\delta p = \delta m(v_R - v_L)$ , must be compensated by an acceleration of the whole plasma to the left, since the hydrodynamic forces are internal, causing an effective gravity

$$g = \rho_- v_- (v_R - v_L)/m \quad (10)$$

This condition determines the approximate slab boundaries, and completes the global description of the laser-plasma interaction. Figure 2 shows the self-consistent profiles and boundaries found by specifying  $I_a$ ,  $I_r$ ,  $m$ ,  $g$ ,  $\rho_c$ , and  $T_c$  only.

Since the jump conditions are not satisfied at the slab boundaries, the steady state assumption breaks down near the boundaries. Equation (10) is good, however, as long as the widths of the unsteady slab ends are much less than the overall width of the slab.

The gravity increases,

$$dg/dt = \rho_- v_- (dv_R^2/dx - dv_L^2/dx)/2m,$$

and can only be considered steady during an interval  $\Delta t$  if

$$\Delta t \ll 2(v_R - v_L)/(dv_R^2/dx - dv_L^2/dx) \quad . \quad (11)$$

If the cold fluid is no wider than about  $T_o/m_i g$ , and the underdense region is wider than about  $T_c/m_i g$ , then (3), (9), and (11) imply a characteristic time scale for growth of the acceleration of  $v_R/g$ . The dynamical development of a slab can be followed over longer time periods by respecifying gravity and intensity if desired, and repeating the integration of (2).

I wish to thank J. P. Boris for valuable comments and suggestion of this topic, and S. E. Bodner and D. L. Book for advice and encouragement.

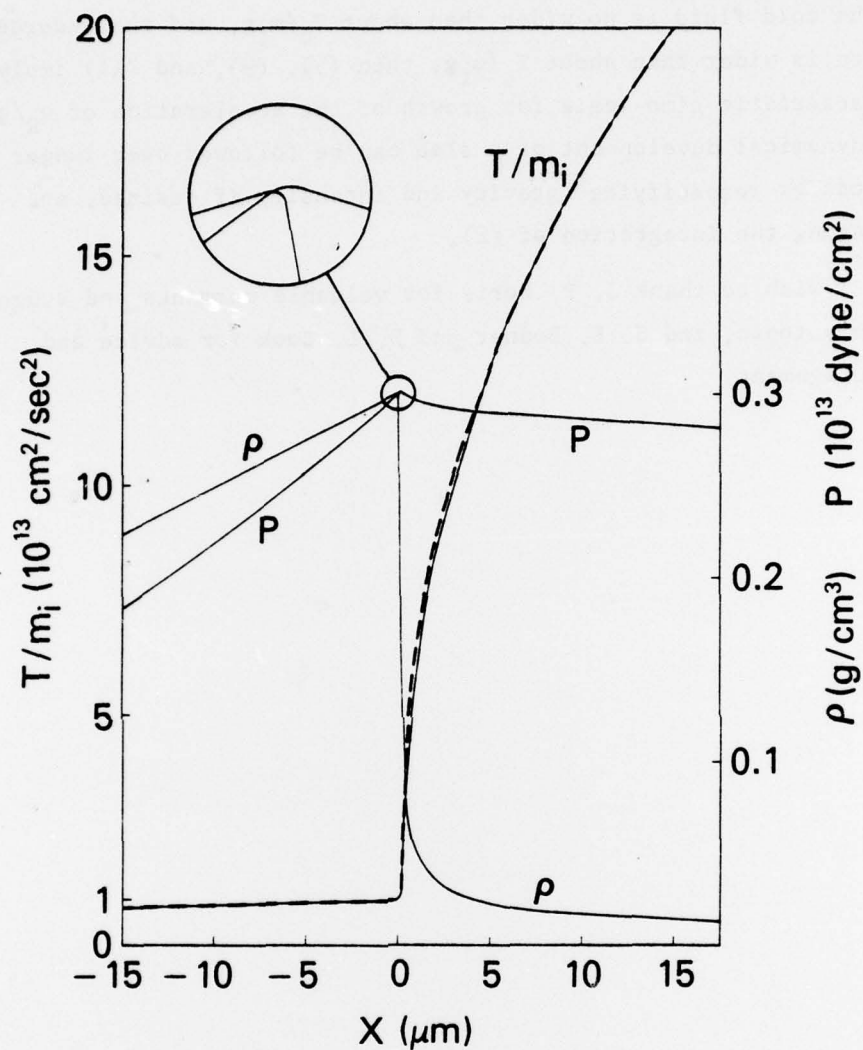


Fig. 1 — Temperature, density, and pressure profiles at ablation layer calculated by model for  $T_o/m_i = 10^{13} \text{ cm}^2/\text{sec}^2$ ,  $v_o = 2.2 \times 10^5 \text{ cm/sec}$ ,  $\rho_o = 0.3 \text{ g/cm}^3$ , and acceleration  $g = 3 \times 10^{15} \text{ cm/sec}^2$ . Dashed curve is analytic temperature approximation (Eqs. (3-4)).



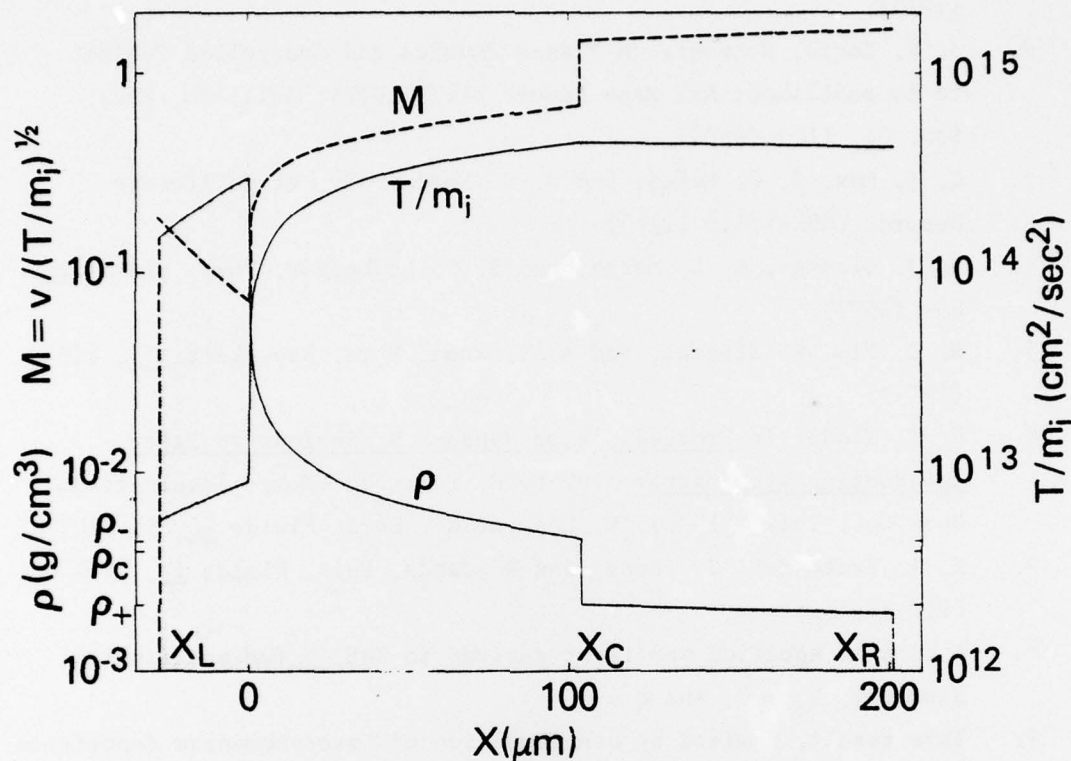


Fig. 2 — Density, temperature, and Mach number profiles of global slab model. Specified were absorbed flux  $I_a = 10.2 \text{ TW/cm}^2$ , reflected flux  $I_r = 10.2 \text{ TW/cm}^2$ , total mass  $m = 0.733 \text{ mg/cm}^2$ , acceleration  $g = 3 \times 10^{15} \text{ cm/sec}^2$ , critical density  $\rho_c = 4 \times 10^{-3} \text{ g/cm}^3$ , and critical temperature  $T_c/m_i = 4.50 \times 10^{14} \text{ cm}^2/\text{sec}^2$ ; coefficient of conductivity  $K = 10^{-33} m_i^{-7/2} \text{ (cgs)}$ . Self consistency of the global model required critical surface at  $x_c$ , left and right boundaries at  $x_L$  and  $x_R$ , and upper and lower shelf densities  $\rho_-$  and  $\rho_+$  shown. No saturation of heat flux occurs here for flux-limit parameter  $\ell > 1.79$ .

#### REFERENCES

1. F. S. Felber and J. H. Marburger, Phys. Rev. Lett. 36, 1176 (1976).
2. J. P. Boris, Comments on Plasma Physics and Controlled Fusion, to be published; NRL Memo Report 3427 (1977); Bull. Am. Phys. Soc. 21, 1103 (1976).
3. C. E. Max, C. F. McKee, and W. C. Mead, Univ. of California Report, UCRL-78458 (1976).
4. S. J. Gitomer, R. L. Morse, and B. S. Newberger, Phys. Fluids 20, 234 (1977).
5. H. C. Kim, R. Stenzel, and A. Y. Wong, Phys. Rev. Lett. 33, 886 (1974).
6. R. E. Kidder in Proceedings of Japan-U.S. Seminar on Laser Interaction with Matter, ed. by C. Yamanaka (Tokyo International Book Co., Tokyo, 1975); K. Lee, et al, Phys. Fluids 20, 51 (1977).
7. K. A. Brueckner, S. Jorna, and R. Janda, Phys. Fluids 17, 1554 (1974).
8. A similar equation was first derived in Ref. 3 for spherical geometry,  $T_0 = 0$ , and  $g = 0$ .
9. This result, implied by consideration of laser-momentum deposition, agrees with Refs. 6 and 10, and is contrary to Ref. 4, in which laser momentum deposition was not treated.
10. K. A. Brueckner and R. S. Janda, to be published.
11. F. C. Young et al., Appl. Phys. Lett. 30, 45 (1977); W. M. Manheimer, D. G. Colombant, and B. H. Ripin, Phys. Rev. Lett. 38, 1135 (1977).

DISTRIBUTION LIST

USERDA (50 copies)  
P. O. Box 62  
Oak Ridge, Tennessee 37830

DDC (20 copies)

National Technical Information Service (24 copies)  
U.S. Department of Commerce  
5285 Port Royal Road  
Springfield, VA 22161

NRL, Code 2628 (35 copies)  
NRL, Code 7700 (25 copies)  
NRL, Code 7730 (50 copies)

USERDA (3 copies)  
Division of Laser Fusion  
Washington, D.C. 20545  
Attn: Dr. C. M. Stickley